

ORGANIC CHEMISTRY

Organic semiconductor photocatalyst can bifunctionalize arenes and heteroarenes

Indrajit Ghosh^{1,2}, Jagadish Khamrai¹, Aleksandr Savateev², Nikita Shlapakov¹, Markus Antonietti^{2*}, Burkhard König^{2*}

Photoexcited electron-hole pairs on a semiconductor surface can engage in redox reactions with two different substrates. Similar to conventional electrosynthesis, the primary redox intermediates afford only separate oxidized and reduced products or, more rarely, combine to one addition product. Here, we report that a stable organic semiconductor material, mesoporous graphitic carbon nitride (mpg-CN), can act as a visible-light photoredox catalyst to orchestrate oxidative and reductive interfacial electron transfers to two different substrates in a two- or three-component system for direct twofold carbon-hydrogen functionalization of arenes and heteroarenes. The mpg-CN catalyst tolerates reactive radicals and strong nucleophiles, is straightforwardly recoverable by simple centrifugation of reaction mixtures, and is reusable for at least four catalytic transformations with conserved activity.

Over the past decade, transition metal complexes (1–3) and organic dyes (4, 5) have been investigated extensively as visible light-absorbing catalysts in a wide range of photoredox transformations (4, 6). Nonetheless, their use is restricted on account of incompatibility with strong acidic or basic reaction media (7), strong nucleophiles, electrophiles, or reactive radical intermediates (4) exemplified by *fac*-Ir(ppy)₃, which reacts with C(sp³) radicals, leading eventually to catalyst deactivation (8, 9). The photophysical properties of organic photocatalysts, such as eosin Y, drastically change with changing pH of the solution (7), and acridinium, triarylpyryliums, and quinolinium dyes are deactivated in the presence of nucleophiles such as amines, acetates, phosphates, or cyanide ions (4, 10, 11).

Organic semiconductor materials are photo- and chemically stable toward otherwise reactive radicals and nucleophiles and have a suitable bandgap between valence band maxima and conduction band minima (12, 13) for controlled oxidation and reduction of many practical substrates. Light absorption by heterogeneous semiconductor photocatalysts generates surface redox centers as electron-hole pairs (14–16). As such, a semiconductor photocatalyst, upon photoexcitation, accomplishes two aligned redox transformations on the same particle surface (14–16), whereas a molecular photocatalyst, after electron transfer to one reaction partner, completes the overall redox process through a subsequent redox reaction of the oxidized or

reduced catalyst. In the latter case, the reactive catalyst intermediate may also engage in unwanted chemical reactions, leading to catalyst decomposition (4, 17). The stability and the aligned interfacial oxidation and reduction, without the generation of reactive catalyst redox intermediates, bestow semiconductor photocatalysts easy control over the primary redox intermediates, which, depending on semiconductor redox reaction modes, affords the final product. Kisch has earlier proposed two different semiconductor reaction modes in visible-light photocatalysis (15, 16, 18): In semiconductor type A photoredox reactions, the intermediates generated by oxidation and reduction lead to two separate products, whereas in semiconductor type B, photocatalysis orchestrated oxidative and reductive redox reactions, allowing both intermediates to participate in yielding the final product. However, a broader appreciation of such semiconductor photocatalytic reaction modes in synthesis was attenuated by the use of toxic metal sulfides as semiconductor photocatalysts, which are photocorrosive (15, 19) under synthetic organic reaction conditions, and only linear sequences of radical or radical ion addition reactions were realized.

We report here the application of organic semiconductor mesoporous graphitic carbon nitride (mpg-CN) as a heterogeneous photoredox catalyst for synthetically important functionalizations of arenes and heteroarenes. Even though the first synthesis of mpg-CN dates back to 1834 (20), its applications as a photocatalyst have only recently received attention, owing to its capacity to split water under visible-light illumination (12, 21, 22). The metal-free, nontoxic (23), straw-yellow powder (24) is easily synthesized in multigram quantities. Although mpg-CN is not commercially available as of yet, the

cost of its straightforward synthesis from readily available starting materials is only a few euros per kg (25) (supplementary materials, materials and methods). The available redox window upon visible-light photoexcitation spans 2.7 V [from approximately +1.2 V to -1.5 V versus saturated calomel electrode (SCE) upon 460-nm illumination], and the electronic band structures can be easily tuned through modification of the nanomorphology or doping (13). This redox window covers a diverse range of redox-active substrates and is comparable to or greater than those of widely used transition metal complexes, organic dyes, and inorganic semiconductors, such as Ru(bpy)₃²⁺, eosin Y, and CdS, respectively (Fig. 1). In suspension, mpg-CN is stable toward reactive nucleophilic, electrophilic, and radical intermediates, as well as acidic and basic conditions (pH range 0 to 14) (12) and intense light irradiation.

Figure 1 summarizes the working strategies of arene C-H functionalizations using mpg-CN as a heterogeneous semiconductor photocatalyst. In these processes, the photogenerated hole and electron on the catalyst surface orchestrate oxidative and reductive redox steps to yield arene products functionalized at two distinct C-H sites from either two or three starting materials. We designate these reactions as type B' and type B'', respectively, to distinguish them from the original process of linear radical combinations described by Kisch (Fig. 1) (15, 16, 18). When the substrate activation leads to monofunctionalized arene products by means of a coupled sacrificial redox process, the processes are classified as oxidative or reductive type A, depending on the redox mode (hole or electron) for substrate activation. Overall, these transformations include direct one-pot dual C(sp²)-C(sp³)/C(sp²)-heteroatom and C(sp²)-C(sp³)/C(sp²)-C(sp³) C-H functionalizations and innate (that is, at the inherently reactive positions) or regiospecific C(sp²)-C(sp³), C(sp²)-C(sp²), or C(sp³)-heteroatom bond-forming reactions resulting in the installation of more than 20 different synthetically important functionalities onto arenes and heteroarenes under oxidative, reductive, or dual catalytic reaction conditions, as well as in the presence of strong nucleophiles, highly reactive sp³/sp² C-centered radicals, and acids or bases.

Bifunctionalization of arenes and heteroarenes by mpg-CN

The synthetic examples of semiconductor photocatalytic arene C(sp²)-C(sp³)/C(sp²)-heteroatom bifunctionalizations at two distinct C-H sites are shown by using alkyl bromides as the source of two different functional groups (Fig. 2). Upon single-electron reduction, the C(sp³)-bromine bond in alkyl bromides breaks spontaneously, generating the relevant alkyl radical and a bromide anion (26) for such bifunctionalizations. In the presence of mpg-CN (27), blue-light irradiation for 4 hours of a reaction mixture containing arene and alkyl bromide [in this case, 1-phenylpyrrole and diethyl bromomalonate as

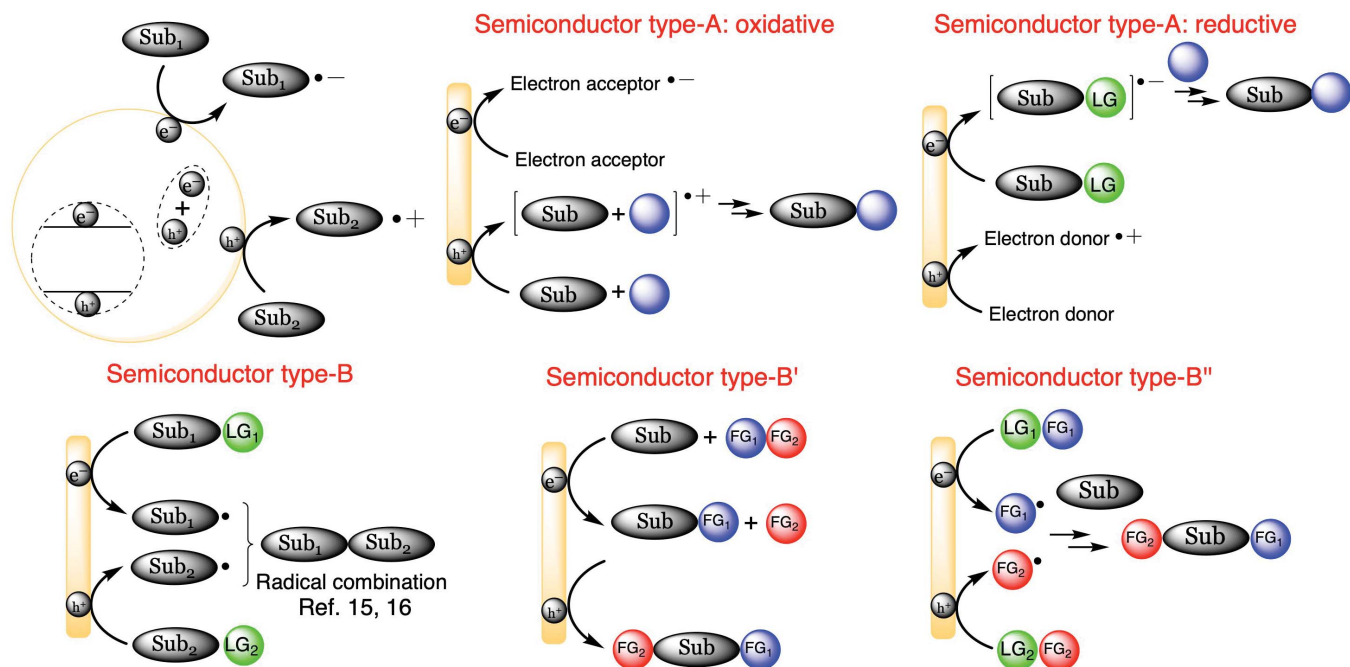
¹Fakultät für Chemie und Pharmazie, Universität Regensburg, 93040 Regensburg, Germany. ²Department of Colloid Chemistry, Max-Planck Institute of Colloids and Interfaces, Research Campus Golm, 14424 Potsdam, Germany. *Corresponding author. Email: markus.antonietti@mpikg.mpg.de (M.A.); burkhard.koenig@ur.de (B.K.)

model substrates (Fig. 2)] yielded the $C(sp^2)-C(sp^3)$ product **1a-1** and $C(sp^2)-Br$ bond-forming product **1a-2** (Fig. 2 and fig. S10) (26, 28). Gas chromatography (GC)-mass spectrometry analysis of the crude reaction mixture revealed the formation of $C(sp^2)-C(sp^3)/C(sp^2)-Br$ bifunctionalized product **1a**. Irradiation of the reaction mixture for longer times led to the formation of the bifunctionalized product **1a** in 63% isolated yield, along with the formation of synthetically important dibrominated arene (**1a-3**, in 27% isolated yield) and $C(sp^2)-C(sp^3)/C(sp^2)-C(sp^3)$ bifunctionalized product **1a-4** as minor product (Fig. 2). The formation of such bifunctionalized arenes that were obtained in excellent overall yield required only mixing of heteroarene, alkyl bromide, and mpg-CN in dimethyl sulfoxide (DMSO) and irradiation under nitrogen with a blue light-emitting diode (LED). Control reac-

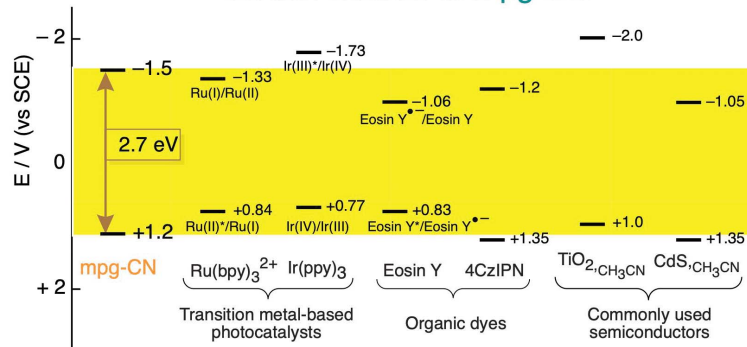
tions (without mpg-CN or no visible-light irradiation) confirmed that photocatalysis by mpg-CN is imperative for the formation of **1a**. Although complex, a likely mechanism for the formation of bifunctionalized product **1a** involves the initial redox-neutral C-H arene alkylation and net oxidative bromination of the arene generating the monofunctionalized products **1a-1** and **1a-2** (chemical structures in Fig. 2), respectively, which upon further redox-neutral or net oxidative redox transformations generate the bifunctionalized products. The net reaction, generating the bifunctionalized product **1a**, can be viewed as the formal insertion of the heteroarene onto a $C(sp^3)-Br$ bond releasing dihydrogen, which, however, was not detected in the head space GC analysis, suggesting the role of excess diethyl bromomalonate as redox and proton balance in the overall transforma-

tion (supplementary materials). A molecular photocatalyst can mediate heteroarene bifunctionalization reactions through the generation of oxidized or reduced catalyst species, and we demonstrated this by using $Ru(bpy)_3^{2+}$ as a photocatalyst yielding product **1a** in approximately 40% GC yield (experimental details in the synthetic procedures section in the supplementary materials). However, the photochemical reaction using eosin Y as a photocatalyst did not give the desired product **1a**. The design of photoredox transformations using a molecular photocatalyst leading to bifunctionalized heteroarenes and the yields of the reaction depend on the stability of the oxidized or reduced photocatalyst after the initial electron transfer in the presence of different reactive intermediates and under photoirradiation, their respective lifetimes, and associated electron

Arene C-H functionalizations using semiconductor photoredox catalytic reaction modes



Redox window of mpg-CN



Photophysical properties of mpg-CN

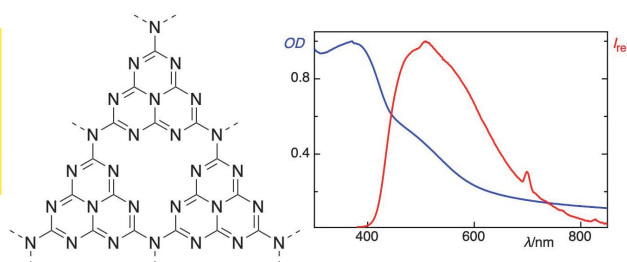


Fig. 1. Schematic representations of semiconductor photoredox catalytic reaction modes in C-H arene functionalizations. The type B' mode can also combine oxidative and reductive photocatalytic steps. Chemical structure, absorption and luminescence spectra, and relative band positions and redox potentials of mpg-CN with respect to commonly applied photocatalysts are shown.

Semiconductor photoredox catalytic arene C–H bifunctionalizations

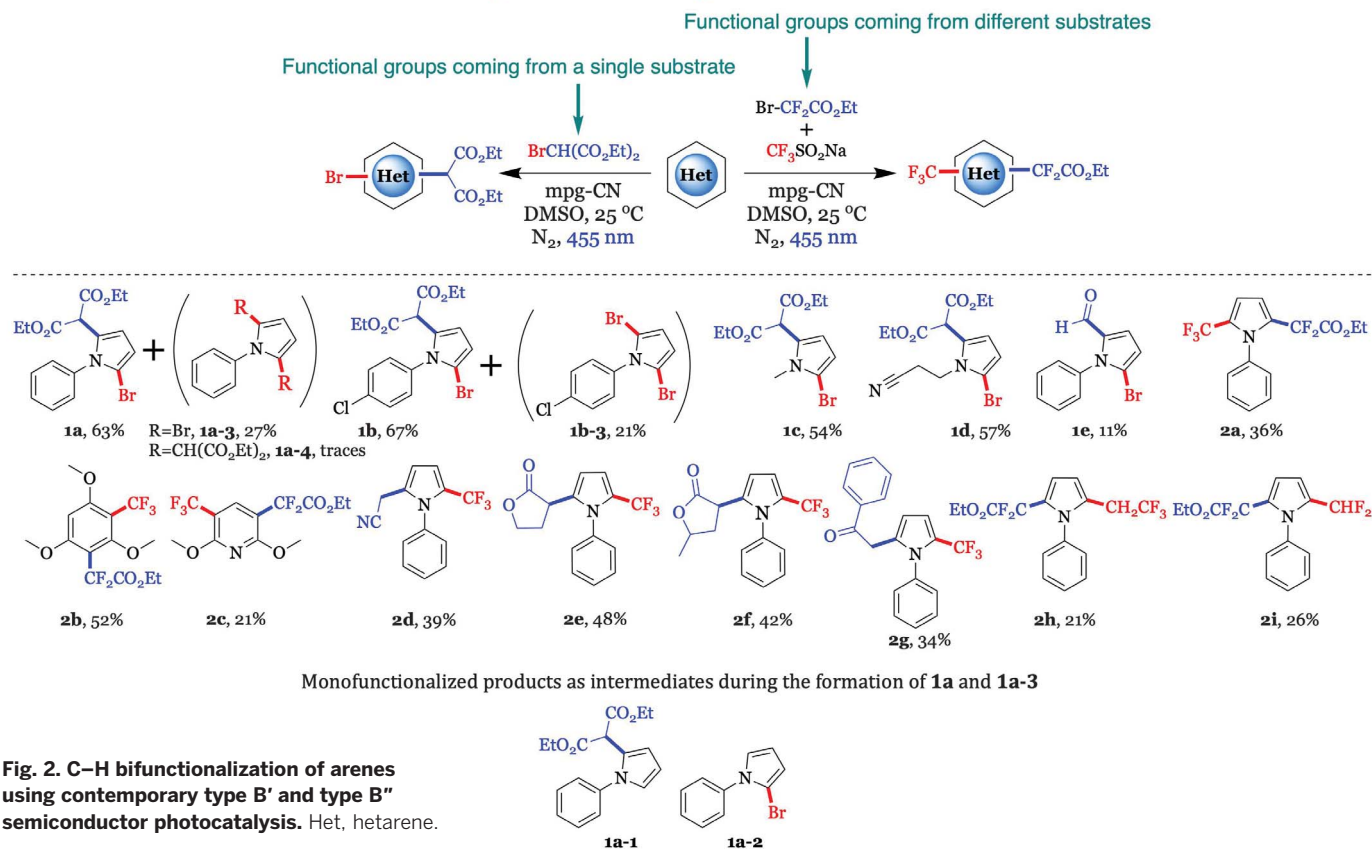


Fig. 2. C–H bifunctionalization of arenes using contemporary type B' and type B'' semiconductor photocatalysis. Het, hetarene.

transfer kinetics to substrates or intermediates. The organic semiconductor mpg-CN, upon photoexcitation, naturally generates electron and hole pairs, and its stability and associated electron-hole transfer kinetics enable easy execution of such bifunctionalizations, with catalyst recoverability and reuse as a practical advantage.

Biologically relevant pyrrole derivatives containing different substituents, such as haloarene, alkyl, or –CN functionalities, were compatible with the reaction conditions, yielding the respective products (**1a–1d**) in moderate-good yields. Commodity chemicals, such as bromoform, were also applicable in these bifunctionalization reactions, affording **1e**, which contains both an aldehyde group and a newly formed C–Br bond.

The formation of such bifunctionalized heteroarenes is an exciting development in photoredox catalysis. Although photocatalytic multitransformations have recently been attempted (29–32), challenges remain in developing methods that allow for a one-pot orchestrated sequential transformation, as established in homogeneous metal, organo-, or enzyme catalysis (33). The few reported examples of photocatalytic tandem and cascade reactions often involve combining photo- and enzymatic catalysis or using cascades that combine different activation modes.

Difficulties arise predominantly from poor photocatalyst compatibility under diverse reaction conditions. The mpg-CN photocatalytic protocol tolerates oxidative and reductive reaction sequences.

The C–H bifunctionalization reaction was extended in scope to C(sp²)–C(sp³)/C(sp²)–C(sp³) bond-forming reactions when we activated the functional groups of different reaction partners by means of complementary redox processes (type B'') in a tricomponent system. In this process, we envision arene bifunctionalizations using two different C(sp³)-centered radicals accessed through oxidative and reductive photoredox transformations. Sodium triflate has an oxidation potential of approximately +1.1 V (versus SCE, table S4) and is oxidized by photoexcited mpg-CN, generating the CF₃SO₂ radical that, upon releasing SO₂, generates a •CF₃ (trifluoromethyl) radical. When a reaction mixture containing arene (in this case, 1-phenylpyrrole as a model substrate), alkyl bromide ethyl bromodifluoroacetate, sodium triflate, and mpg-CN was illuminated using a blue LED, the twofold C–H functionalized product **2a** was obtained in 36% isolated yield along with synthetically important monofunctionalized products (separate trifluoromethylated arene and alkylated arene: fig. S12). In typical semiconductor type B photocatalysis (15) or in conventional “paired electro-

synthesis (34),” the primary redox intermediates (radicals or radical ions) that are generated by oxidative and reductive redox steps combine to give coupled end products. Our reaction, described as semiconductor type B'', orchestrated the reaction of two redox intermediates with one arene, forming two new chemical bonds (Fig. 2). Although the isolated yields of the bifunctionalized products are only moderate to good, the clean conversion, simple operation, and facile separation and isolation of the products recommend the mpg-CN catalyzed arene C(sp²)–C(sp³)/C(sp²)–C(sp³) bond-forming bifunctionalization protocol for applications in organic synthesis. Among other investigated substrates, ethyl bromodifluoroacetate, bromoacetone, α-bromo-γ-butyrolactone, substituted α-bromo-γ-butyrolactone, and phenacyl bromide were effective precursors of functionally important alkyl, (substituted) γ-butyrolactone, and phenacyl radicals. Reactions with these radicals yielded the corresponding bifunctionalized products **2a–g** in moderate to good isolated yields considering two new C–C bond-forming reactions. Similarly, using this mpg-CN photoredox catalytic protocol, the scope of oxidative partners was easily extended, allowing installation of medicinally relevant –CH₂CF₃ (**2h**) and difluoromethyl (–CF₂H, **2i**) groups. The –CH₂CF₃ group is slightly electron withdrawing and an

excellent bioisostere of an ethyl group, and the $-\text{CF}_2\text{H}$ group is a lipophilic hydrogen bond donor and acts as a bioisostere for alcohol and thiol functional groups.

Although a detailed mechanistic picture of these transformations remains to be elucidated, the experimental results suggest that sodium triflate, in addition to being the source of the $\bullet\text{CF}_3$ radical, competed effectively with other oxidation processes. Irradiation of arene substrates (for example, 1-phenylpyrrole and 1,3,5-trimethoxybenzene) in the presence of only ethyl bromodifluoroacetate yielded monofunctionalized C–C (examples **6d** and **6a** in Fig. 3) and brominated arenes (by means of C–Br bond formation; chemical structures in table S5) as separate products. However, in the presence of sodium triflate, the bifunctionalized products **2a** and **2b** were obtained in 36% and 52% isolated yields, respectively (Fig. 2). Similar observations were found for other oxidative partners in their respective reactions.

Direct C–H monofunctionalizations of arenes and heteroarenes by mpg-CN

The mpg-CN semiconductor photocatalysis is highly effective for direct C–H functionalizations of arenes in the presence of “sacrificial” electron donors or acceptors, operating then through a more conventional type A reaction mode (Fig. 1). Whereas C–H functionalizations of arenes are reported using conventional photocatalysts (4, 6, 10, 11, 35), the photocatalyst selection and synthetically demanding catalyst modification for a given transformation (11) still remain a fundamental challenge in photoredox catalysis. Photocatalyst deactivation (8, 11) limits the direct use of many unprotected strong nucleophiles in arene C–H functionalizations (10), catalyst reuse in large-scale synthetic transformations, or orchestrated sequential transformations under diverse redox reaction conditions using different reagents (for example, nucleophiles and reactive radicals in a sequence, Fig. 5) in one-pot sequential catalytic reactions. As we discuss in the following sections, mpg-CN semiconductor photocatalytic reactions proceed through the generation of reactive C-centered sp^3 or sp^2 radicals from the respective radical precursors under both oxidative and reductive reaction conditions (Fig. 3) or in the presence of reactive nucleophiles, ideally bulk chemicals such as alkali metal salts (Fig. 4).

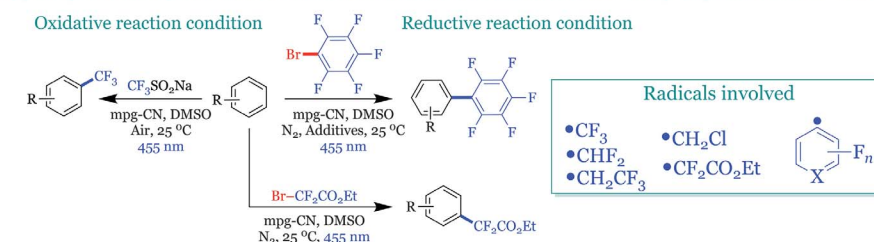
C–H arene functionalizations using radical precursors

Examples of C–H arene functionalizations using $\text{C}(\text{sp}^3)$ - and $\text{C}(\text{sp}^2)$ -centered radicals under oxidative and reductive semiconductor type A photoredox reaction conditions are shown in Fig. 3. In particular, the $\bullet\text{CF}_3$, $\bullet\text{CH}_2\text{CF}_3$, $\bullet\text{CF}_2\text{H}$, or pentafluoro aryl $\bullet\text{C}_6\text{F}_5$ radical sources have been recently used extensively for late-stage functionalizations of medicinally relevant molecules (36–39). Irradiation of a reaction mixture containing 1,3,5-trimethoxybenzene (model

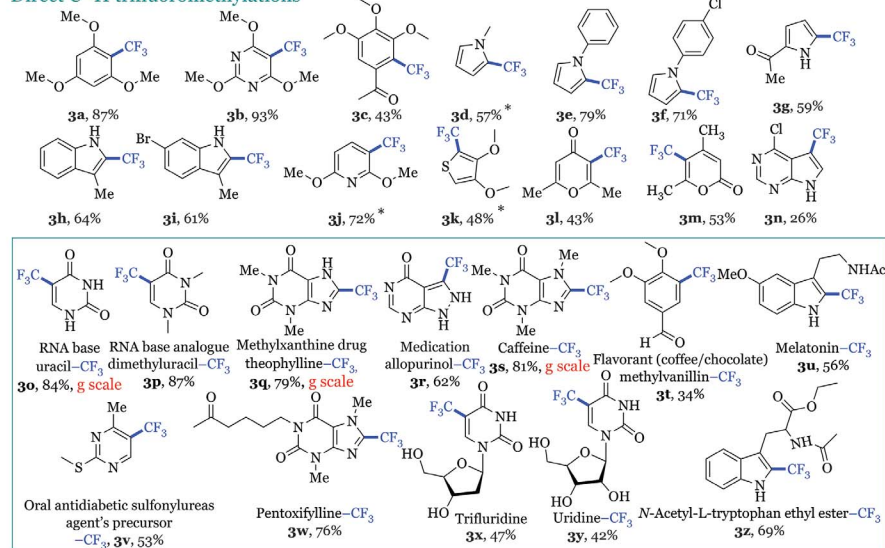
substrate), mpg-CN, and the commercially available trifluoromethanesulfinic acid sodium salt under air led to the formation of the corresponding trifluoromethylated product **3a** in 87% isolated yield. Trifluoromethyl radical couplings to boronic acids (36) or unactivated arenes (37, 38) are typically performed using difficult-

to-handle trifluoroiodomethane (a toxic gas) or trifluoromethanesulfonyl chloride (a corrosive low-boiling liquid). These reactions are performed under strictly inert conditions by using transition metal catalysts. Alternatively, sodium triflate reactions have required an excess of peroxides as radical initiators that

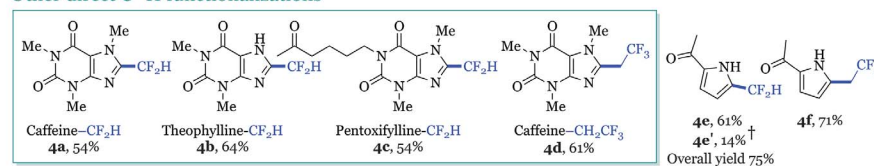
Type A photocatalytic direct C–H functionalizations of (het)arenes via sp^2/sp^3 C-centered radicals



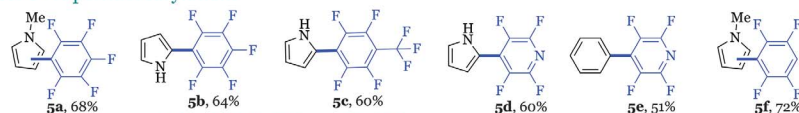
Direct C–H trifluoromethylations



Other direct C–H functionalizations



Direct C–H perfluoroarylations



Direct C–H difluoroalkylations

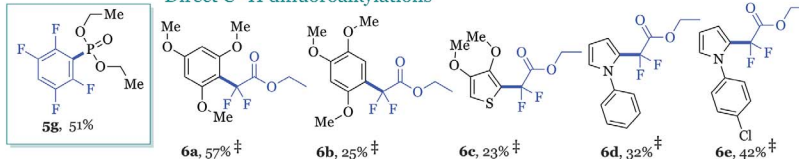


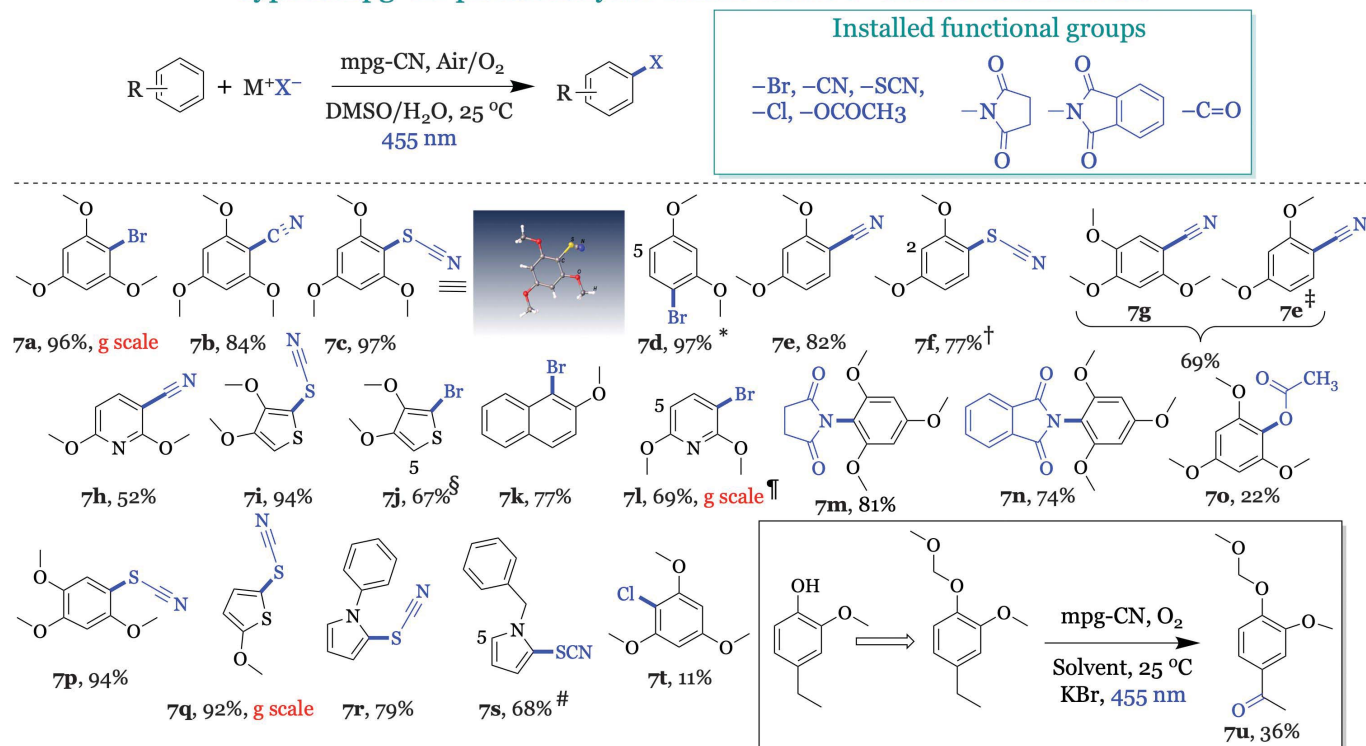
Fig. 3. Direct C–H trifluoromethylations, difluoromethylations, perfluoroarylations of arenes, and medicinally relevant molecules by means of oxidative or reductive radical reactions. *NMR yield by ^{19}F NMR. †The bifunctionalized product was obtained in 14% isolated yield. ‡Respective bromoarene was formed as the major by-product (table S5). NMR, nuclear magnetic resonance.

need careful controlled addition at a larger scale. In contrast, trifluoromethylation reactions using mpg-CN work in the presence of air, and the catalyst is easily recovered for reuse (Fig. 5). Control reactions confirmed that the presence of mpg-CN and light irradiation were crucial for successful direct C–H transformations of arenes (table S2). Under the optimized reaction condition, a range of five- and six-

membered heteroarenes, such as pyrimidines (**3b**), pyrroles (**3d** to **3g**), indoles (**3h** and **3i**), pyridines (**3j**), thiophenes (**3k**), 7-deazapurine (**3n**), and medicinally relevant arenes [for example, veratraldehyde (**3t**), widely used as a flavorant or odorant], were cleanly converted to their respective trifluoromethylated products in good to excellent yields. Pharmaceuticals, hormones, and bioactive molecules, including the

RNA base uracil (**3o**), 1,3-dimethyluracil (**3p**), theophylline (**3q**, respiratory disease medication), allopurinol (**3r**, uric acid medication), caffeine (**3s**), melatonin (**3u**, hormone), 4-methyl-2-(methylthio)pyrimidine (**3v**, oral antidiabetic sulfonylureas agent's precursor), pentoxifylline (**3w**, muscle pain medication), uridine (**3y**), and tryptophan (**3z**), all showed excellent reactivity toward trifluoromethylation,

Type A mpg-CN photocatalysis: Innate direct C–H functionalizations



Ligand free organic semiconductor (mpg-CN)/Ni dual catalytic C–X functionalizations

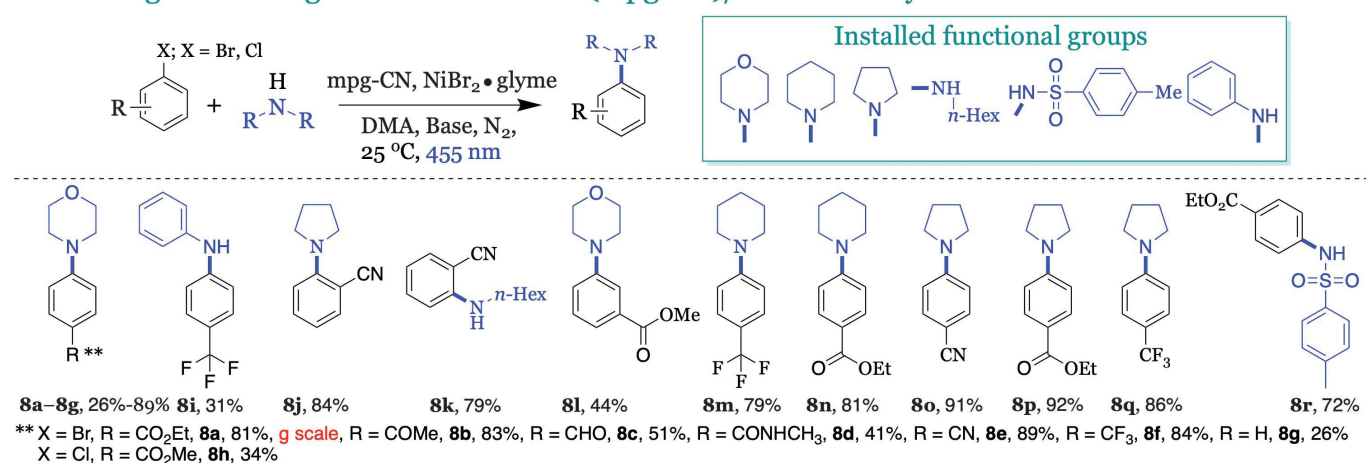


Fig. 4. C–H and C–X (where X = Br, Cl) functionalizations of arenes at room temperature using alkali metal salts and ligand-free mpg-CN/Ni dual photoredox catalytic protocols, respectively. The reactions were carried out using mpg-CN as a heterogeneous photocatalyst and a blue LED. *The bisubstituted product was

obtained in 12% isolated yield. †Positional isomers: 16:1. ‡Ipsio substitution product. §The bifunctionalized product was obtained as a major product. ¶The bisubstituted product (**7l'**) was formed in minimal amount. **7l:7l'** = 16:1. #The bisubstituted product was obtained in 11%.

yielding the respective products, including the synthesis of trifluridine (**3x**), in good to excellent yields. Similar reactivity and product yields were obtained when the reactions were performed on gram scales (examples **3o**, **3q**, **3s** in Fig. 3). Similarly, the installation of difluoromethyl ($-\text{CF}_2\text{H}$) and $-\text{CH}_2\text{CF}_3$ groups onto caffeine (**4a**, **4d**), theophylline (**4b**), pentoxifylline (**4c**), and pyrrole derivatives (**4e-4f**) yielded the desired products in good to excellent yields (Fig. 3).

The C-H arene functionalizations using $\text{C}(\text{sp}^2)$ -centered radicals under reductive type A photocatalytic reaction conditions was demonstrated through synthetically important direct C-H perfluoroarylations of arenes through the activation of $\text{C}(\text{sp}^2)$ -bromine bonds in perfluoroaryl bromides. Upon photoexcitation, mpg-CN has a reduction potential of approximately -1.5 V (versus SCE) and can therefore assist mesolytic cleavage of the $\text{C}(\text{sp}^2)$ -Br bonds in polyfluoroaryl bromides (reduction potentials in table S4) through a single-electron transfer, catalyzing direct C-H perfluoroarylations of arenes (**5a** to **5f**). When triethylphosphite was present in the reaction mixture, reductive formation of $\text{C}(\text{sp}^2)$ -P bonds was observed (**5g**, Fig. 3, 51% isolated yield).

C-H arene functionalizations using nucleophiles

Examples of direct $\text{C}(\text{sp}^2)$ -H arene functionalizations using reactive nucleophiles are de-

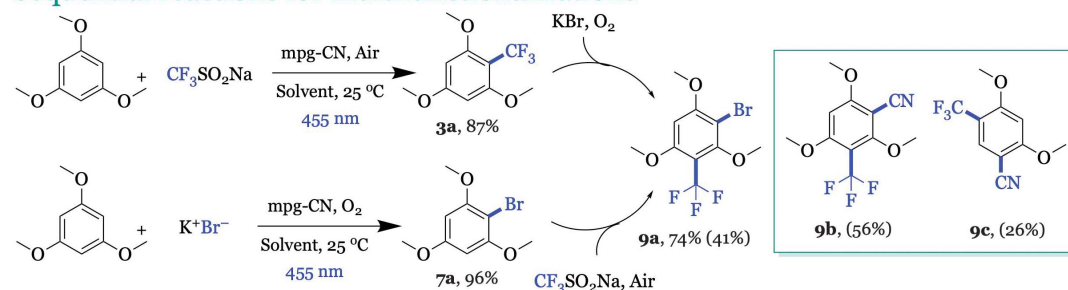
scribed in Fig. 4. Simple inorganic or organic alkali metal salts served as precursors for the desired functional groups for direct C-H functionalizations of arenes that encompassed brominations, relatively less explored thiocyanations, and in particular cyanations. These reactions involve just mixing of substrates, the respective alkali metal salts, and mpg-CN, followed by solvent addition and blue-light illumination of the reaction mixture under air (or with an oxygen balloon; materials and methods). Previously described methods for arene cyanations required slow-releasing cyanide precursors, such as trimethylsilyl cyanide in photocatalytic reactions using acridinium (*10*) and palladium catalysts (*40*), as the cyanide ion deactivates both palladium(II) and palladium(0) species in the catalytic cycle (*40*). These limitations are not observed when mpg-CN is used. Conducting the reactions in the absence of light, oxygen, or mpg-CN did not afford the desired products in reasonable yields (table S3). Several substituted arenes (including naphthalene, **7k**) and various functionalized six- or five-membered heteroarenes—such as pyridine (**7h**, **7l**) or thiophenes (**7i** to **7j**, **7q**) and pyrroles (**7r** and **7s**), which are prone toward polymerization under oxidative reaction conditions—proceeded under our conditions to afford the respective C-H functionalized products in good to excellent yields (Fig. 4). Arenes could also be substituted by using small molecules with relatively acidic protons such as succinimide

or phthalimide (**7m** and **7n**, through the formation of C-N bonds) or salts such as acetate (**7o**, through the formation of C-O bond). The succinimide group serves as a versatile amine equivalent, as the respective products can be easily transformed into the corresponding amines (*41*). The chlorination reaction using NH_4Cl led to the formation of product **7t** (Fig. 4). These reactions are easily performed on large scales (gram-scale reaction in examples **7a**, **7l**, and **7q** in Fig. 4), and the mpg-CN catalyst also withstood high-power blue-light illumination when the reaction was performed in a high-light-intensity photoreactor with radiant flux of $2.0 \pm 0.3\text{ W}$ (for comparison, the radiant flux of a typical commercial single-spot LED is $0.5 \pm 0.1\text{ W}$). Entry 3 in table S3 and fig. S1 present the respective photochemical reaction yield and high-light-intensity reaction setup), under which many conventional photocatalysts bleach (*42*).

C-X arene functionalizations

The examples discussed so far (Figs. 2 to 4) showcase C-H arene functionalization at their inherently reactive positions. Slightly altered semiconductor/Ni dual catalytic reaction conditions allow the regioselective arene functionalization through the activation of $\text{C}(\text{sp}^2)$ -X (where X = Br, Cl) bonds in electron-poor aryl halides. Dual photo-nickel catalysis with conventional photocatalysts, typically iridium complexes (*43*, *44*), has evolved over the past several years

Sequential reactions for multifunctionalizations



Catalyst recycling

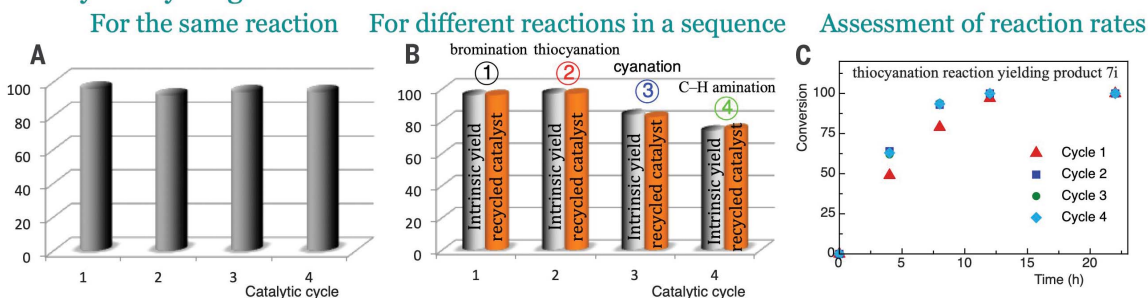


Fig. 5. Sequential reactions and evaluation of catalytic recycling. (A and B) Evaluation of catalyst recycling either for the same (in this case a bromination reaction yielding product **7a**) or different reactions (in this case, consecutive bromination, thiocyanation, cyanation, and C-H amination reactions performed in a sequence yielding products **7a**, **7c**, **7b**, and **7n**, respectively). (C) Kinetic profile of a photocatalytic

transformation (in this case, the thiocyanation reaction yielding product **7i**) over four catalytic cycles. The simplicity of the synthetic gram-scale reactions (in this case trifluoromethylation of caffeine) using mpg-CN as a photocatalyst are depicted in (D, E, and F): (D) required reagents and reaction setup; (E) photochemical reaction setup under visible-light illumination; (F) isolated product (product **3s**) and the recovered photocatalyst.

into a valuable synthetic tool for cross-coupling (45). The use of mpg-CN as a semiconductor photocatalyst allows catalyst recoverability and reuse as a distinct advantage. The reaction conditions require no additional ligands for nickel complexation, the reactions proceed at room temperature, and the chemical and photostability of mpg-CN allows easy scalability to gram quantities (example **8a**). Once dissolved in dimethylacetamide (DMA), ethyl 4-bromobenzoate irradiated with blue light in the presence of morpholine (a heterocycle featuring both amine and ether functional groups), mpg-CN, and a catalytic amount $\text{NiBr}_2 \cdot \text{glyme}$ was converted into the corresponding C–N functionalized product in 81% isolated yield. The use of *o*–/*m*–/*p*–substituted aryl bromides (or even chlorides, example **8h**) yielded the corresponding regio-specific functionalized products in good to excellent yields, and different functional groups, such as ester, aldehyde, ketone, amide, trifluoromethyl, and cyano, were tolerated under the reaction condition. The mpg-CN/Ni dual catalytic reactions are effective for various nitrogen nucleophiles (examples **8a** to **8q**), including substituted benzenesulfonamide providing the corresponding *N*-aryl sulfonamide (**8r**) [a motif present in pharmaceuticals (46)], in good to excellent yields.

Recoverability and reuse of mpg-CN

The use of insoluble heterogeneous semiconductor mpg-CN as a photocatalyst and its photo- and chemical stability facilitate easy recovery of the catalyst from a wide variety of reaction mixtures, including gram-scale and dual catalytic reactions, by simple centrifugation (Fig. 5) or filtration (fig. S14). The recovered catalyst could be reused for multiple transformations with conserved activity, as specifically appraised by determining the product yields over four catalytic cycles either for the same reaction (Fig. 5A) or for different reactions performed in a sequence (Fig. 5B); rates of photocatalytic transformations (47, 48) over four catalytic cycles were also conserved (Fig. 5C). The photocatalyst's high stability enables one-pot sequential type A oxidative direct C–H bifunctionalizations of heteroarenes in the presence of reactive $\text{C}(\text{sp}^3)$ radicals and strong nucleophiles. This is exemplified by consecutive trifluoromethylation and bromination reactions that led to the formation of the

bifunctionalized product **9a** in 74% yield (Fig. 5). This sequential reaction simply required the addition of KBr and continuous irradiation once the trifluoromethylation reaction was complete. Likewise, when sodium triflate was added post cyanation (examples **9b** and **9c**), the bifunctionalized products containing $-\text{CF}_3$ and $-\text{CN}$ groups were obtained.

Considering all of these results in aggregate, the organic semiconductor mpg-CN stands out as one of the most versatile visible light-activated photocatalysts, providing an inexpensive, non-toxic alternative to classical transition metal catalysts and organic dyes.

REFERENCES AND NOTES

1. C. K. Prier, D. A. Rankic, D. W. C. MacMillan, *Chem. Rev.* **113**, 5322–5363 (2013).
2. M. H. Shaw, J. Twilton, D. W. C. MacMillan, *J. Org. Chem.* **81**, 6898–6926 (2016).
3. D. A. Nicewicz, D. W. C. MacMillan, *Science* **322**, 77–80 (2008).
4. N. A. Romero, D. A. Nicewicz, *Chem. Rev.* **116**, 10075–10166 (2016).
5. I. Ghosh, T. Ghosh, J. I. Bardagi, B. König, *Science* **346**, 725–728 (2014).
6. I. Ghosh, L. Marzo, A. Das, R. Shaikh, B. König, *Acc. Chem. Res.* **49**, 1566–1577 (2016).
7. M. Majek, F. Filice, A. J. von Wangelin, *Beilstein J. Org. Chem.* **10**, 981–989 (2014).
8. J. J. Devery III et al., *Chem. Sci.* **6**, 537–541 (2015).
9. C. J. O'Brien et al., *J. Org. Chem.* **83**, 8926–8935 (2018).
10. J. B. McManus, D. A. Nicewicz, *J. Am. Chem. Soc.* **139**, 2880–2883 (2017).
11. N. A. Romero, K. A. Margrey, N. E. Tay, D. A. Nicewicz, *Science* **349**, 1326–1330 (2015).
12. X. Wang et al., *Nat. Mater.* **8**, 76–80 (2009).
13. Y. Wang, X. Wang, M. Antonietti, *Angew. Chem. Int. Ed.* **51**, 68–89 (2012).
14. D. Friedmann, A. Hakkii, H. Kim, W. Choi, D. Bahnemann, *Green Chem.* **18**, 5391–5411 (2016).
15. H. Kisch, *Angew. Chem. Int. Ed.* **52**, 812–847 (2013).
16. H. Kisch, *Acc. Chem. Res.* **50**, 1002–1010 (2017).
17. J. P. Dinnozeno et al., *J. Am. Chem. Soc.* **111**, 8973–8975 (1989).
18. W. Schindler, H. Kisch, *J. Photochem. Photobiol. Chem.* **103**, 257–264 (1997).
19. J. L. DiMeglio, B. M. Bartlett, *Chem. Mater.* **29**, 7579–7586 (2017).
20. J. B. Liebig, *Ann. Pharm.* **10**, 10 (1834).
21. For previous use of mpg-CN in synthetic transformations by Antonietti, Blechert, Wang, and others, see (22).
22. A. Savateev, I. Ghosh, B. König, M. Antonietti, *Angew. Chem. Int. Ed.* **57**, 15936–15947 (2018).
23. A. W. Wang, C. D. Wang, L. Fu, W. N. Wong-Ng, Y. C. Lan, *Nano-Micro Lett.* **9**, 21 (2017).
24. Morphology and other information about mpg-CN are available in the supplementary materials.
25. Y. Dai et al., *Nat. Commun.* **9**, 60 (2018).
26. L. Furst, B. S. Matsuura, J. M. R. Narayanan, J. W. Tucker, C. R. J. Stephenson, *Org. Lett.* **12**, 3104–3107 (2010).
27. The catalyst loading discussion is provided in the synthetic procedures section in the supplementary materials.

28. K. Ohkubo, K. Mizushima, R. Iwata, S. Fukuzumi, *Chem. Sci. (Camb.)* **2**, 715–722 (2011).
29. Z. C. Litman, Y. Wang, H. Zhao, J. F. Hartwig, *Nature* **560**, 355–359 (2018).
30. J. B. Metternich, R. Gilmour, *J. Am. Chem. Soc.* **138**, 1040–1045 (2016).
31. M. J. James, J. L. Schwarz, F. Strieth-Kalthoff, B. Wibbeling, F. Glorius, *J. Am. Chem. Soc.* **140**, 8624–8628 (2018).
32. J. Hou et al., *J. Am. Chem. Soc.* **140**, 5257–5263 (2018).
33. Y. Hayashi, *Chem. Sci.* **7**, 866–880 (2016).
34. C. Amatore, A. R. Brown, *J. Am. Chem. Soc.* **118**, 1482–1486 (1996).
35. J. M. R. Narayanan, C. R. J. Stephenson, *Chem. Soc. Rev.* **40**, 102–113 (2011).
36. Y. Ye, M. S. Sanford, *J. Am. Chem. Soc.* **134**, 9034–9037 (2012).
37. Y. Ji et al., *Proc. Natl. Acad. Sci. U.S.A.* **108**, 14411–14415 (2011).
38. D. A. Nagib, D. W. C. MacMillan, *Nature* **480**, 224–228 (2011).
39. S. Senaweera, J. D. Weaver, *J. Am. Chem. Soc.* **138**, 2520–2523 (2016).
40. M. Sundermeier, S. Mutyala, A. Zapf, A. Spannenberg, M. Beller, *J. Organomet. Chem.* **684**, 50–55 (2003).
41. K. Foo, E. Sella, I. Thomé, M. D. Eastgate, P. S. Baran, *J. Am. Chem. Soc.* **136**, 5279–5282 (2014).
42. S. Schmidbauer, A. Hohenleutner, B. König, *Beilstein J. Org. Chem.* **9**, 2088–2096 (2013).
43. J. C. Tellis, D. N. Primer, G. A. Molander, *Science* **345**, 433–436 (2014).
44. E. B. Corcoran et al., *Science* **353**, 279–283 (2016).
45. J. Twilton et al., *Nat. Rev. Chem.* **1**, 0052 (2017).
46. T. Kim, S. J. McCarver, C. Lee, D. W. C. MacMillan, *Angew. Chem. Int. Ed.* **57**, 3488–3492 (2018).
47. S. L. Scott, *ACS Catal.* **8**, 8597–8599 (2018).
48. C. W. Jones, *Top. Catal.* **53**, 942–952 (2010).

ACKNOWLEDGMENTS

We thank R. Vasold, R. Hoheisel, and J. Zach for GC-MS, CV measurements, and technical assistance, respectively, and R. Lahmy for proofreading the manuscript. **Funding:** We thank the Deutsche Forschungsgemeinschaft (GRK 1626 and DFG An 156 13-1) for financial support. This project also received funding from the European Research Council (ERC) under the European Union's Horizon 2020 research and innovation program (grant agreement no. 741623). **Author contributions:** B.K. and M.A. conceived and directed the project. I.G., B.K., M.A., J.K., A.S., and N.S. designed the experiments. I.G., J.K., A.S., and N.S. performed and analyzed the experiments. I.G., B.K., M.A., J.K., and A.S. prepared the manuscript. **Competing interests:** The authors declare no conflicts of interest. **Data and materials availability:** Crystallographic parameters for compound **7c** are available free of charge from the Cambridge Crystallographic Data Centre under CCDC 1880753. Data are available in the supplementary materials.

SUPPLEMENTARY MATERIALS

science.sciencemag.org/content/365/6451/360/suppl/DC1
Materials and Methods
Figs. S1 to S23
Tables S1 to S7
References (49–105)

9 December 2018; accepted 3 June 2019
10.1126/science.aaw3254

Organic semiconductor photocatalyst can bifunctionalize arenes and heteroarenes

Indrajit Ghosh, Jagadish Khamrai, Aleksandr Savateev, Nikita Shlapakov, Markus Antonietti and Burkhard König

Science **365** (6451), 360-366.
DOI: 10.1126/science.aaw3254

Two-for-one approach to photoredox

In photoredox catalysis, an excited chromophore typically activates a single reactant either by oxidizing or reducing it. Ghosh *et al.* used a semiconductor catalyst to activate two reactants at once by quenching both an excited electron and the residual positive hole (see the Perspective by Swift). As such, two different reactive carbon or halide fragments could be appended to separate sites on an aryl ring. The catalyst also tolerated strong nucleophiles such as cyanide and could be recovered easily and reused.

Science, this issue p. 360; see also p. 320

ARTICLE TOOLS

<http://science.sciencemag.org/content/365/6451/360>

SUPPLEMENTARY MATERIALS

<http://science.sciencemag.org/content/suppl/2019/07/24/365.6451.360.DC1>

RELATED CONTENT

<http://science.sciencemag.org/content/sci/365/6451/320.full>

REFERENCES

This article cites 104 articles, 6 of which you can access for free
<http://science.sciencemag.org/content/365/6451/360#BIBL>

PERMISSIONS

<http://www.sciencemag.org/help/reprints-and-permissions>

Use of this article is subject to the [Terms of Service](#)

Science (print ISSN 0036-8075; online ISSN 1095-9203) is published by the American Association for the Advancement of Science, 1200 New York Avenue NW, Washington, DC 20005. The title *Science* is a registered trademark of AAAS.

Copyright © 2019, American Association for the Advancement of Science